

# Genetic and Functional Analyses Point to *FAN1* as the Source of Multiple Huntington Disease Modifier Effects

Kyung-Hee Kim,<sup>1,2</sup> Eun Pyo Hong,<sup>1,2</sup> Jun Wan Shin,<sup>1,2</sup> Michael J. Chao,<sup>1,2</sup> Jacob Loupe,<sup>1,2</sup> Tammy Gillis,<sup>1</sup> Jayalakshmi S. Mysore,<sup>1</sup> Peter Holmans,<sup>3,4</sup> Lesley Jones,<sup>3,4</sup> Michael Orth,<sup>4,5</sup> Darren G. Monckton,<sup>4,6</sup> Jeffrey D. Long,<sup>4,7,8</sup> Seung Kwak,<sup>4,9</sup> Ramee Lee,<sup>9</sup> James F. Gusella,<sup>1,4,10,11</sup> Marcy E. MacDonald,<sup>1,2,4,10</sup> and Jong-Min Lee<sup>1,2,4,10,\*</sup>

A recent genome-wide association study of Huntington disease (HD) implicated genes involved in DNA maintenance processes as modifiers of onset, including multiple genome-wide significant signals in a chr15 region containing the DNA repair gene Fanconi-Associated Nuclease 1 (*FAN1*). Here, we have carried out detailed genetic, molecular, and cellular investigation of the modifiers at this locus. We find that missense changes within or near the DNA-binding domain (p.Arg507His and p.Arg377Trp) reduce *FAN1*'s DNA-binding activity and its capacity to rescue mitomycin C-induced cytotoxicity, accounting for two infrequent onset-hastening modifier signals. We also identified a third onset-hastening modifier signal whose mechanism of action remains uncertain but does not involve an amino acid change in *FAN1*. We present additional evidence that a frequent onset-delaying modifier signal does not alter *FAN1* coding sequence but is associated with increased *FAN1* mRNA expression in the cerebral cortex. Consistent with these findings and other cellular overexpression and/or suppression studies, knockout of *FAN1* increased CAG repeat expansion in HD-induced pluripotent stem cells. Together, these studies support the process of somatic CAG repeat expansion as a therapeutic target in HD, and they clearly indicate that multiple genetic variations act by different means through *FAN1* to influence HD onset in a manner that is largely additive, except in the rare circumstance that two onset-hastening alleles are present. Thus, an individual's particular combination of *FAN1* haplotypes may influence their suitability for HD clinical trials, particularly if the therapeutic agent aims to reduce CAG repeat instability.

## Introduction

Huntington disease (HD; MIM: 143100) is due to an expanded (>35) CAG trinucleotide repeat in *HTT* (MIM: 613004)<sup>1</sup> that encodes a lengthened polyglutamine segment in the large huntingtin protein. The HD mutation precipitates a constellation of neurological symptoms (e.g., involuntary movements, psychiatric disturbances, and cognitive decline)<sup>2</sup> and leads to premature death.<sup>3</sup> Both age at onset of characteristic motor signs and age at death show a strong inverse correlation with *HTT* CAG repeat length,<sup>4–7</sup> but there is remaining variance that shows heritability, indicating that in addition to *HTT*, other genes play a role in determining the exact course of HD in any given individual. To identify genetic factors that modify HD age at onset, the GeM-HD Consortium carried out an initial genome-wide association study (GWAS) of ~4,000 HD subjects, and the study revealed three genome-wide significant onset-modification signals, including two opposing modifier signals at 15q13.2–13.3.<sup>8,9</sup> Recently, an expanded GWAS of ~9,000 HD subjects showed that the timing of HD

onset is due to a length-dependent property of the expanded CAG repeat rather than to polyglutamine size, and that the effects of this property are modified by at least six loci that harbor genes involved in DNA repair and/or maintenance processes.<sup>10</sup> Together, these findings point to somatic CAG repeat expansion as the likely mechanism that determines age at onset, suggesting this process as a target for therapeutic intervention to delay or prevent HD onset. A detailed understanding of the modification effects could also underpin the use of genetic modifier genotype in clinical trial inclusion criteria and/or outcome analysis.

Among other genes, the 15q13.2–13.3 modifier locus contains Fanconi-Associated Nuclease 1 (*FAN1*; MIM: 613534), which encodes a protein that participates in DNA interstrand cross-link (ICL) repair, and there is some support from model systems for reduced *FAN1* levels resulting in trinucleotide repeat instability.<sup>11,12</sup> The recent GWAS produced evidence of additional onset modifier signals in this region and suggested that onset-hastening and onset-delaying signals might be respectively associated with *FAN1* missense variants that are potentially

<sup>1</sup>Molecular Neurogenetics Unit, Center for Genomic Medicine, Massachusetts General Hospital, Boston, MA 02114, USA; <sup>2</sup>Department of Neurology, Harvard Medical School, Boston, MA 02115, USA; <sup>3</sup>Medical Research Council Centre for Neuropsychiatric Genetics and Genomics, Department of Psychological Medicine and Neurology, School of Medicine, Cardiff University, Cardiff CF24 4HQ, UK; <sup>4</sup>The GeM-HD consortium, <sup>5</sup>Department of Neurology, University of Ulm, Ulm 89081, Germany; <sup>6</sup>Institute of Molecular, Cell and Systems Biology, College of Medical, Veterinary and Life Sciences, University of Glasgow, Glasgow G12 8QQ, UK; <sup>7</sup>Department of Biostatistics, College of Public Health, University of Iowa, Iowa City, Iowa 52242, USA; <sup>8</sup>Department of Psychiatry, Carver College of Medicine, University of Iowa, Iowa City, Iowa 52242, USA; <sup>9</sup>CHDI Foundation, Princeton, NJ 08540, USA; <sup>10</sup>Medical and Population Genetics Program, the Broad Institute of M.I.T. and Harvard, Cambridge, MA 02142, USA; <sup>11</sup>Department of Genetics, Blavatnik Institute, Harvard Medical School, Boston, MA 02115, USA

\*Correspondence: [jlee51@mgh.harvard.edu](mailto:jlee51@mgh.harvard.edu)

<https://doi.org/10.1016/j.ajhg.2020.05.012>

© 2020 American Society of Human Genetics.

deleterious and with eQTLs that increased *FANI* mRNA levels in the cerebral cortex.<sup>10</sup> To test these predictions and to better inform potential HD intervention strategies, we have explored this chromosome (chr) 15 locus and its modifier signals in greater detail, using molecular, cellular, and genetic strategies.

## Material and Methods

### Subjects and Phenotype

HD subjects for our initial onset modifier genome-wide association (GWA) analysis (namely GeM-HD GWA123)<sup>9</sup> and additional HD subjects for our second GWA analysis (namely GeM-HD GWA12345) were described previously.<sup>10</sup> Age at onset of motor symptoms was based mainly on rater's estimation; if such data were not available, we then used age-at-onset data in the clinical records or provided by family members or subjects. A stringent and robust phenotyping model for calculating individual deviation of age at onset from the expected age at onset based on one's expanded CAG repeat length was described previously.<sup>6</sup> This residual age at onset, representing the age at onset that was not explained by the CAG repeat size, was the primary phenotype used for genetic analysis. HD subjects with positive and negative residual age at onset developed motor symptoms later or earlier than expected, respectively. For example, a HD participant with residual age at onset of 10 means that the subject developed motor symptoms 10 years later than expected based on one's expanded CAG repeat length. The distribution of residual age at onset of motor symptoms of study subjects was very similar to a theoretical normal distribution, allowing standard statistical analyses.<sup>10</sup> Subject consents and the overall study design were reviewed and approved by the Partners HealthCare Institutional Review Board.<sup>10</sup>

### Genotype Imputation and Association Analysis Using the Quantitative Residual Age-at-Onset Phenotype

Subjects were genotyped in five HD modifier GWA studies as described previously.<sup>10</sup> In order to obtain genotype data with the highest SNP density for the current study, we performed two independent genotype imputations using 1000 Genomes Project (KGP) data (phase 3, mixed population) and Haplotype Reference Consortium (HRC, European) as the reference panels using the Michigan Imputation Server. Each typed GWA data set was subjected to extensive quality control analyses implemented by the Michigan Imputation Server, and genotype imputation was carried out using EAGLE for the phasing and MINIMAC3 for the imputation. The two independent sets of imputed genotype data were then merged by supplementing HRC imputation data with KGP imputation-specific data. In the end, 9,058 samples<sup>10</sup> were imputed for analysis in this study (4,414 males and 4,644 females). Because mixed-effect models generated similar results to those generated by fixed-effect models (data not shown), all SNPs (except 32 SNPs with imputation call rate < 100%) were analyzed to determine the level of association between the minor allele count of a test SNP (additive model) and the residual age at onset of subjects in a fixed-effect model. Each fixed-effect model for a given test SNP also included a set of covariates such as GWA study, sex, and the four top ancestry characteristics obtained from multidimensional scaling (MDS) analysis using genome-wide typed data with the PLINK program (version 1.07). After considering

the patterns of association signals and recombination rate, our analysis focused on the chr15: 30900000–31500000 region. Low-performing SNPs (5,206) were flagged (e.g., minor allele frequency [MAF] < 0.01%, Hardy-Weinberg equilibrium p value <  $1 \times 10^{-6}$ , or mean imputation R square values < 0.5). MAF data were based on imputed genotype data of the study subjects. Details of the original chr15 modifier haplotype-tagging SNPs are described elsewhere.<sup>10</sup> Genomic coordinates were based on the GRCh37/hg19 assembly.

### CNV Analysis

Genotype intensity files were processed by using the PENNCNV program to determine copy number variation (CNV) genotypes. We performed quality control (QC) analysis by taking CNV segments that (1) were greater than 10 KB in size and (2) were determined by more than 10 sites. Frequencies of CNV (duplication and deletion) were calculated based on study subjects. Overall CNV frequencies are very low in the region—124 subjects carry CNVs in the chr15 region—so we performed association analysis using the residual age-at-onset phenotype and excluding these subjects in order to judge the impact of CNVs on the observed SNP association signals. To test whether increased dosage of *FANI* affects age at onset, the residual age at onset of HD subjects carrying three copies of *FANI* was compared to that of HD subjects with two copies of *FANI*. Statistical significance of increased *FANI* copy number was evaluated by an ANOVA model with the same covariates that were used in SNP association analysis.

### Nomenclature of Modifier Haplotypes

To clarify each modifier haplotype on chr15, we used a naming system that was used previously.<sup>10</sup> In brief, the first number represents chromosome number, the letter "M" stands for modifier, the next letter indicates the order of discovery ("A" represents the first modifier locus in that chromosome), and the last number is given to distinguish apparent independent modifier effects at the locus. Although the 15AM4 haplotype was originally thought to represent a single independent modifier effect, further analysis here indicates that this haplotype captures multiple separate modifier effects, leading us in this study to focus on 15AM1, 15AM2, 15AM3, and 15AM5, each of which appears to capture a single independent modifier effect.

### Construction of Nucleotide-Resolution Modifier Haplotypes Using KGP Data

We constructed full-length modifier haplotypes based on haplotype-tagging SNPs and KGP data (phase 3). KGP chromosomes carrying the modifier haplotypes were identified based on refined modifier haplotype-tagging SNPs (15AM1, 3; 15AM2, 46; 15AM3, 3; and 15AM5, 2; refer to Table S2). Then the most frequent alleles at each site in the KGP chromosomes were taken as the consensus alleles of each modifier haplotype. Subsequent analysis was focused on modifier haplotype boundaries defined by the haplotype-tagging SNPs. Next, we split the variation sites in the reconstructed haplotypes into two groups depending on whether or not SNPs were tested in our association analysis. For SNPs that we tested and that are also annotated in the KGP, we evaluated whether functional changes in proteins contributed to modification signals. Similarly, we examined annotations of SNPs that were not tested in our analysis but were described in the KGP data set in order to judge a possibility of modification of HD due to functional changes in proteins.

## Functional Annotation of SNPs

SNPs were annotated based on the ExAC database in order to identify variations with functional impact; we focused on (1) protein-altering variations and (2) deleterious mutations. Protein-altering variants included SNPs annotated as frameshift variants, in-frame deletions, in-frame insertions, missense variants, protein-altering variants, splice acceptor variants, splice donor variants, start lost, stop gained, or stop lost.

## Supplemental Targeted Capture Sequencing Analysis and Genotype-based Analysis

In order (1) to confirm functional variations in the modifier haplotypes identified by KGP haplotype analysis, (2) to detect variations that were not annotated in KGP, and (3) to investigate their roles in modifying HD, we performed targeted capture sequencing analysis of selected representative HD samples carrying modifier haplotypes. Previously described haplotype-tagging SNPs were used to select samples for capture sequencing. Using the Agilent SureDesign online tool, capture probes were designed to enrich the target region (chr15: 31050000-31314317); tiling probes were designed to cover each base pair position by five independent probes. This generated ultra-long 120-mer biotinylated complementary RNA baits, and these capture probes were used for solution-based SureSelect target enrichment.<sup>13</sup> In brief, genomic DNAs were sheared to produce smaller fragments, and libraries were prepared with sequence-specific adaptors and indexes for multiplexing. DNA libraries were hybridized with biotinylated cRNA baits, which were complementary to regions to capture. The bait-library complexes were pulled down by magnetic beads. After the beads were washed, the RNA bait was digested to obtain the target DNA and was subjected to sequencing using Illumina HiSeq 100bp paired-end sequencing at the Broad Institute. Samples were independently captured and/or indexed, and all capture materials were pooled together for sequencing in a single lane. Sequence reads were aligned (using Burrows-Wheeler Aligner [BWA] and Picard) for variant calling using the Genome Analysis Toolkit Best Practices workflow. At least 2.5 million sequence reads were produced for each sample, generating mean coverage of ~167×. Called variations were compared to KGP data. For shared variation sites between KGP data and our capture sequencing data, we evaluated the allele frequency of functional variations identified from KGP haplotype analysis to confirm the presence of functional variations with expected frequencies. For capture-sequencing-specific variations, we focused on exon variations with expected allele frequency of the causal variation.

## eQTL Analysis Using the CommonMind Consortium Data and Co-localization Analysis

We obtained genotype and expression data from the CommonMind Consortium (CMC) in order to compare significances of SNPs in HD modifier association analysis with those in gene-level eQTL analysis results. A standard eQTL analysis was performed by modeling expression levels of *FAN1* as a function of a test SNP (additive model), MDS covariates, and sex in a fixed-effect model. SNPs in 1MB flanking regions of *FAN1* were tested (2,732 SNPs in 451 samples including 269 males). Then SNPs were matched between HD GWA analysis and CMC eQTL analysis based on chromosome, genomic location (GRCh37/hg19), reference allele, and alternative allele. 1,840 SNPs were shared by HD GWA data and CMC eQTL data, and were subsequently compared. Co-localization analysis was based on 'coloc' R package (version 3.2-1) in

the R environment. Posterior probability of (1) causal variant for HD modifier trait only, (2) causal variant for CMC eQTL trait only, and (3) one common causal variant were calculated by 'coloc.abf' function using summary data for HD GWAS and CMC eQTL.

## Cell Culture

HEK293T cells and *FAN1* knockout HEK293T cells were cultured in DMEM (Invitrogen) supplemented with 10% fetal bovine serum (Hyclone) and Penicillin-Streptomycin (Invitrogen) at 37°C and 5% CO<sub>2</sub>. Lymphoblastoid cell lines (LCLs) derived from HD subjects were cultured in RPMI (Sigma-Aldrich) supplemented with 5% fetal bovine serum and Penicillin-Streptomycin at 37°C and 5% CO<sub>2</sub>.

## *FAN1* Knockout HEK293T Cells

To obtain modifier *FAN1* protein extracts without endogenous *FAN1*, we inactivated endogenous *FAN1* in the HEK293T cells through the use of the CRISPR/Cas9 approach. A *FAN1*-specific gRNA (target site, chr15:31206161-31206180) was selected from the GeCKO library,<sup>14,15</sup> and potential off-target sites were checked in the Optimized CRISPR design website. Annealed oligos were inserted into the lentiCRISPR V2 vector (Addgene, 52961) as recommended on the GeCKO website.<sup>14,15</sup> HEK293T cells were then transfected with *FAN1*-targeting CRISPR/Cas9 plasmid using Lipofectamine 2000 (Invitrogen). After selection with 1 µg/ml of Puromycin (Invitrogen) for 48 h, single cells were picked and independently expanded to establish clonal lines. Two lines were developed and further analyzed via Sanger sequencing. The levels of *FAN1* protein were evaluated via immunoblot analysis (*FAN1* antibody, Abcam, ab95171) using whole cell lysate (50 µg). The location of a *FAN1* protein band in the immunoblot analysis was confirmed through the use of *FAN1*-overexpressed samples.

## Cloning of *FAN1* Modifier Haplotypes and Generation of Full-length cDNA Expression Vectors

We selected a panel of HD LCLs to generate full-length *FAN1* expression vectors; cells were selected based on the genotypes of haplotype-tagging SNPs (rs150393409 for 15AM1; rs35811129 for 15AM2). Total RNA samples were prepared using the RNeasy Plus mini kit (Qiagen), and cDNA was subsequently prepared using the SuperScript III first-strand kit (Invitrogen). The concentration and purity of DNA and RNA samples were determined using NanoDrop (ND-1000). We used cDNA to amplify full-length 15AM1 and 15AM2 *FAN1* (primers, 5'-GGCGGCCGCAATGATGTCAGAAGGGAAACCTCCTGAC-3' and 5'-CAGATCTTTAGCTAAGGCTTTGGCTCTTAGCTCCAAC-3'). Amplified DNA was isolated from the agarose gel and extracted for digestion by NotI and BglII. Digested DNA was inserted into a linearized FLAG-tagged mammalian expression vector (pFLAG-CMV-4 expression vector; Sigma-Aldrich, E7158). The vector for 15AM3 was generated by site-directed mutagenesis using the 15AM2 plasmid. For all plasmids, the full sequence was verified through the use of Sanger sequencing analysis. Our *FAN1* plasmids confirmed the sequences reconstructed from KGP haplotype analysis and supplemental capture sequencing analysis.

## Qualitative Detection of Interaction between *FAN1* and 3' Flap DNA Substrate

To qualitatively assess whether *FAN1* protein interacts with 3' flap DNA substrate, we performed EMSA (electrophoretic mobility shift assay)-type assays. Our 3' flap DNA substrate consisted of

oligonucleotides that have been used previously in a crystal structure study, and showed a strong binding affinity to FAN1.<sup>16</sup> The constituents of this complex are: (1) a 40-nucleotide-long oligo with biotin at the 5' end (5'-CCCCTCCAGTCTCGTCCGC GCCACTCGTGTCCAGCGTCG-3'; namely Biotin-A1), (2) a post-nick probe with 5'-phospho (5'-TGCGGACGAGACCTGGACG GG-3'; namely B2), and (3) a pre-nick oligo (5'-CGACGCTGGA CACGAGTGGCTTTTTTTT-3'; namely C3).<sup>16</sup> These three oligos were annealed by incubating at 95°C for 5 min and gradually cooling to 4°C in annealing buffer (10 mM Tris, 1 mM EDTA, 50 mM NaCl, pH 8.0).<sup>16</sup> Annealing reaction included 5 femtomol of A1, 10 femtomole of B2, and 10 femtomole of C3 in 50 µl of annealing buffer. Figure S7A shows sequences and a conceptual illustration of the annealed oligos. To detect interaction between FAN1 and DNA substrate, nuclear extracts obtained from HEK293T cells or *FAN1* knockout HEK293T cells (prepared by the NE-PER Nuclear and Cytoplasmic Extraction Reagent; Pierce, 78833) were incubated with annealed DNA oligos; 10 µg of nuclear extract were incubated with annealed DNA oligos in 25 mM Tris-HCl pH 7.5, 150 mM NaCl, 50 ng/µl Poly (dI•dC), 5% glycerol, 0.1 mg/ml BSA, 10 mM CaCl<sub>2</sub>, and 0.1 mM DTT at 4°C for 30 min. The binding mixtures were then resolved on 5% Tris-borate-EDTA (TBE) gels (Bio-Rad), and FAN1-DNA substrate interaction was detected using the Biotin-Streptavidin Detection Kit (Pierce, 20148). FAN1-DNA substrate interaction was also confirmed based on an excess amount (1,000×) of non-labeled DNA oligo complex (competitor comprising non-biotinylated A1, B2, and C3). Due to the low performance of a commercially available anti-FAN1 antibody, super shift assay was not performed.

### Quantitative Evaluation of DNA-Binding Activities of Modifier FAN1

To determine the levels of DNA-binding activity of specific modifier haplotype FAN1 protein, we performed quantitative pull-down assays. The same oligo annealing procedures were performed to generate a 3' flap structure except for the amounts of oligos; we incubated 10 picomole of biotinylated A1 (Biotin-A1), 20 picomole of B2, and 20 picomole of C3 in a 30 µl reaction volume. 10 µl of annealed oligos (i.e., 3' flap DNA substrate) was used for each reaction with nuclear lysate. To generate modifier FAN1 protein, *FAN1* knockout HEK293T cells were transfected with *FAN1* expression vectors for 72 h (Lipofectamine 2000), and nuclear extracts were prepared (NE-PER Nuclear and Cytoplasmic Extraction Reagent; Pierce, 78833). 100 µg of individual nuclear extract was used for binding with DNA substrate in 300 µl of binding buffer (PBS, pH 7.4, protease inhibitors; on ice). FAN1-DNA complex was then incubated with 30 µl of Dynabeads MyOne Streptavidin (Invitrogen) at room temperature for 90 min.<sup>17</sup> After washing with PBS (three times), the FAN1-DNA complex was dissociated through the use of 0.1% SDS in NuPAGE LDS (lithium dodecyl sulfate) Sample Buffer (Invitrogen) and resolved on NuPAGE gels (Thermo; 4–12% Bis-Tris Protein Gel). The amount of FAN1 pulled down by 3' flap DNA was determined through the use of an immunoblot assay by anti-FAN1 antibody (Abcam ab95171). Densitometric quantification of bands was performed using Multi Gauge version 2.3 (Fujifilm). The quality of nuclear extracts was evaluated using Lamin A/C in the input (Cell Signaling, #4777; data not shown). FAN1 DNA-binding activity data were normalized based on the amount of FAN1 in the input. In addition, DNA-binding activity of different modifier FAN1 was determined using annealed oligos hypothesized to

form a DNA hairpin/loop structure. To generate CAG-repeat-induced DNA hairpin/loop structures, we used CAG repeat oligos (5'-CGACGCTGGACACGAGTGGC-[CAG]*n*-GCGGACGAGACCT GGACGGG-3'), where *n* = 0, 2, 4, 6, 8, or 10 CAGs inserted into the reverse complementary sequence of Biotin-A1. We annealed these oligos to Biotin-A1 (using the same procedures as above) in order to generate a complex of Biotin-A1 and CAG repeat oligos with CAG loop-outs with the potential to form hairpins. To check the annealed oligos, we incubated 5 femtomol of Biotin-A1 and 10 femtomol of CAG repeat oligo in 50 µl of annealing buffer. The annealed oligos were resolved on 5% TBE gels and detected through the use of the Biotin-Streptavidin Detection Kit. For quantitative DNA-binding assays, we annealed 10 picomole of Biotin-A1 and 20 picomole of CAG repeat probe in a 36 µl reaction volume. 10 µl of annealed oligos was incubated with overexpressed FAN1 nuclear lysate (100 µg). Procedures for binding, streptavidin pull-down, and data normalization were the same as those in assays using a 3' flap DNA substrate. Nuclease activity was not determined in these assays because these assay conditions were not optimal for measuring FAN1 catalytic activity, and the genetic investigation suggested a role for altered DNA binding or expression levels rather than FAN1 catalytic activity.<sup>12</sup>

### Effects of Modifier FAN1 on Cytotoxicity Induced by Mitomycin C (MMC)

We determined whether our modifier *FAN1* expression vectors could rescue MMC-mediated cytotoxicity in the absence of endogenous *FAN1* in HEK293T cells. In brief, *FAN1* knockout HEK293T cells were transfected with *FAN1* overexpression vectors (Invitrogen, Lipofectamine 2000, 72 h). Then, *FAN1* knockout HEK293T cells and *FAN1*-overexpressing knockout HEK293T cells were treated with either dimethyl sulfoxide (DMSO) or MMC (10 µM for 24 h; Abcam). Cell viability of *FAN1*-deficient cells was determined via CellTiter-Glo luminescent cell viability assay (Promega). Each condition was tested in five wells, and the entire experiments were repeated four times each. We also determined whether HD LCLs with different modifier *FAN1* haplotypes show different sensitivity to this DNA-damaging agent. Ten different HD LCLs were used: (1) five lines carrying one copy of 15AM1 *FAN1* (*HTT* CAG: 37, 41, 41, 41, 53) and (2) five LCLs carrying at least one copy of 15AM2 (*HTT* CAG: 41, 42, 49, 52, 53). HD LCLs were plated in 96-well plates at  $2 \times 10^4$  cells per well and treated with MMC for 48 h. Cell viability was determined using the CellTiter-Glo Luminescent Cell Viability Assay. For each concentration, six wells were used, and four independent experiments were performed.

### FAN1 Knockout HD iPSC and CAG Repeat Expansion Assay

To examine the effect of *FAN1* knockout on CAG expansion, we used an induced pluripotent stem cell (iPSC) line derived from an HD subject fibroblast (GM04723) with 72 and 15 CAG repeats and two copies of onset-delaying modifier haplotype 15AM2<sup>10</sup> generated as described by the HD iPSC Consortium.<sup>18</sup> Cells were maintained in mTeSR1 with 5X supplements (Stemcell technologies, 85850) at 37°C and 5% CO<sub>2</sub>. The size of a normal CAG repeat is expected to be 15 in all cells, but the length of an expanded CAG repeat may differ from 72 in individual clones due to low-level repeat mosaicism. To generate *FAN1* knockout in these iPSCs, cells were treated 10 µM of Rho-associated, coiled-coil containing protein kinase (ROCK) inhibitor (Millipore,

688000) 1 h before transfection with *FAN1*-specific gRNA containing pLentiCRISPR V2 plasmid and empty vector through the use of the Amaxa Human Stem Cell Nucleofactor Kit 1 (Lonza, VPH-5012). After selection with Puromycin (0.2 µg/ml for 48 h; Invitrogen), single cells were picked and independently maintained. From these, two knockout iPSC clonal lines were generated and respectively confirmed via Sanger sequencing (one nucleotide insertion and eight nucleotide deletions in knockout clonal line #1; one nucleotide insertion and two nucleotide deletions in knockout clonal line #2). The control and knockout cells all showed similar growth rates (data not shown). Genomic DNAs from each iPSC clonal cell line were collected monthly for 6 months (DNeasy, Qiagen) for PCR amplification with HD-CAG-repeat-specific primers.<sup>19</sup> The distribution of CAG repeats in the bulk DNA was determined through the use of a standardized fragment-based genotyping assay using an ABI3730XL sequencer, and the CAG expansion index was calculated from GeneMapper traces as previously described, with a threshold of 10% relative to the maximum height peak.<sup>19</sup>

### Immunoblot Assay

Cells were washed three times with PBS and incubated in cell lysis buffer (Cell Signaling, #9803) containing protease inhibitors (Roche, #11697498001). Protein lysate was separated on 4–12% Bis-Tris gel (Invitrogen) and transferred to polyvinylidene fluoride (PVDF) membranes. After blocking in 5% milk in tris-buffered saline (TBS) containing 0.1% Tween-20, the membranes were incubated overnight at 4°C with primary antibodies. The following primary antibodies were used: anti-FAN1 (Abcam, ab95171), anti-FLAG (Sigma-Aldrich, F1804), and anti-actin (Sigma-Aldrich, A4700). After washing, the blots were probed with anti-mouse, or anti-rabbit IgG-HRP secondary antibodies and visualized via electrochemiluminescence (ECL; PerkinElmer).

### Programs and Statistics

R (version 3.3.3) was used for plotting unless otherwise specified. R 3.5.3 was used for the co-localization analysis. For human *FAN1* molecular and cell experiments, the values are expressed as the mean ± standard error of independent experiments. For group comparisons, Student's *t* tests were performed.

## Results

### Definition of Modifier Signals

The most recent GWAS of ~9,000 HD subjects that implicated multiple significant modifier signals (two infrequent haplotypes: 15AM1 and 15AM3 and two frequent haplotypes: 15AM2 and 15AM4) included 1,963 QC-passed SNPs which were imputed in the chr15:30,900,000–31,500,000 region (GRCh37/hg19) through the use of the Haplotype Research Consortium (HRC) as a reference panel.<sup>10</sup> To achieve a more comprehensive high-density definition of these modifier signals, we have augmented the analysis to now include 13,294 variants in this region by adding short genetic variations (SGVs; including both SNPs and indels) imputed using the KGP as reference panel (Figure S1). Association analysis using residual age at onset of motor signs (i.e., age at onset corrected for individual

CAG repeat size) as the phenotype revealed robust onset modification signals that crossed *FAN1* and also revealed two additional protein coding genes (*MTMR10* and part of *TRPM1*) (Figure 1). Of the 13,294 imputed SGVs, 148 were protein-altering (i.e., frameshift, in-frame deletion, in-frame insertion, missense, splice acceptor, splice donor, start lost, stop gained, or stop lost), and some of these were predicted to be deleterious (Table S1). Two, rs150393409 and rs151322829, represent the *FAN1* missense changes, p.Arg507His and p.Arg377Trp, which are reported to tag the 15AM1 and 15AM3 modification signals, respectively (Figure 1, red triangles).

To test the degree of independence of all modifier signals, we carried out association analyses in which we conditioned separately on each of the modifier-tagging SNPs defining 15AM1, 15AM2, 15AM3, and 15AM4 (Figure S2). The results indicated that the significance of the tag SNPs for each of the first three signals was little affected by conditioning on each other, whereas significance of the 15AM4 tag SNP was respectively increased and decreased by conditioning on the 15AM1 and 15AM2 signals. Reciprocally, conditioning on the 15AM4 tag SNP respectively increased and decreased the significance of 15AM1 and 15AM2 tag SNPs. Thus, the very frequent 15AM4 tag SNP does not in fact capture a single discrete modifier effect but rather a combination of modifier effects; consequently, we excluded it from subsequent analyses in order to delineate individual modifier signals. Because both 15AM1 and 15AM3 signals are captured by infrequent alleles (respectively, ~1.4% and ~0.7% frequency in the study population), we next removed the 381 subjects carrying either of these tag SNPs to simplify more detailed analyses (namely, drop-out analysis). We then repeated the association analysis with this slightly reduced sample size ( $n = 8,677$ ) (Figure 2A). After removal of the onset-hastening signals, the association analysis no longer identified rs35811129 (Figure 2A) as best capturing the onset-delaying 15AM2 signal, but rather pointed to the indel variant rs66632437 ( $p$  value =  $1.3 \times 10^{-25}$ ) and SNP rs8034856 ( $p$  value =  $1.4 \times 10^{-25}$ ) as better tags of this modifier effect. Because indels are not imputed with the HRC reference data, we chose rs8034856 (Figure 2A) as the new tag SNP for analyses of 15AM2. Conditioning on this new 15AM2 tag SNP revealed a previously unrecognized genome-wide significant modifier signal (Figure 2B), which we have termed 15AM5 (Figure 2A, cyan). This third onset-hastening modifier effect is tagged by rs79213781, with a MAF of ~1.9% (effect size, -2.55/year/minor allele). Conditional analysis of each of the 15AM1, new 15AM2, 15AM3, and 15AM5 tag SNPs confirmed 15AM5 to be separate from the previously defined modifier signals (Figure S3). Repeating the association analysis after removal of samples carrying any of 15AM1, 15AM3, or 15AM5 tag SNPs and conditioning on the new 15AM2 peak SNP revealed only signals with  $p$  values  $< 5 \times 10^{-04}$  (data not shown), suggesting that any additional signals which emerge as significant with a further increase in

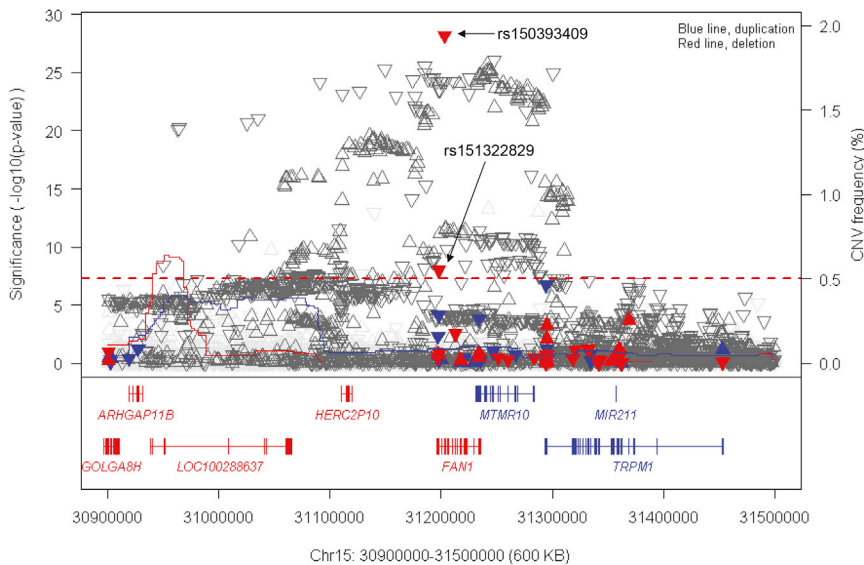


**Figure 1. Dense SGV Marker Association with Residual Age at Onset at the Chromosome 15 HD Modifier Locus**

All SGVs (dark grey, QC-passed; light grey, QC-failed), merged from two sets of imputed genotype data, were evaluated for the levels of association with residual age at onset. For each test variant, the residual age at onset as a continuous phenotype was modeled as a function of minor allele count (additive model), sex, ancestry characteristics, and study group in a fixed-effect model. Y-axis and X-axis represent the levels of significance of association and genomic coordinate (GRCh37/hg19), respectively. Upward and downward triangles represent SNPs whose minor alleles are associated with delayed and hastened age at onset, respectively. Filled blue and red triangles represent protein-altering variants, and the latter are predicted to be deleterious and/or damaging. Traces in blue and red represent the frequencies of duplication and deletion from the CNV

analysis of the study samples (secondary Y-axis). All RefSeq transcripts for a given gene were combined to show locations of exons (vertical bars) and introns; gene symbols in red and blue represent genes on plus and minus strands, respectively. In the region of genome-wide significant signal, only *FAN1*, *MTMR10*, and *TRPM1* are protein-coding genes. Two genome-wide significant and deleterious missense SNPs are indicated by black arrows.

GWAS sample size will represent low-frequency alleles. Finally, conditioning on all independent modifier haplotypes (15AM1, 15AM2, 15AM3, and 15AM5) eliminated all signal detected by 15AM4 (Figure S4).

In addition to the SGV association results, Figure 1 also shows the frequency of CNVs across the region. CNVs were seen in only 124 of 9,058 HD subjects (a low overall frequency in the study population), and these did not align with the patterns of SGV association signals (Figure 1). Exclusion of HD subjects with CNVs had a minimal impact on single-SGV association analysis (Figure S5A), this result indicates that CNV is not responsible for any of the individual 15AM1, 15AM2, 15AM3, or 15AM5 modifier signals. However, eight subjects who each carried three complete copies of *FAN1* showed delayed onset ( $p = 0.016$ ) compared to those without CNV (Figure S5B); this result supports the possibility that in HD, increased *FAN1* levels are protective.

### Construction of Nucleotide-Resolution Modifier Haplotypes and Functional Annotation

For each individual modifier effect, we defined the extent of the chr15 region that contains the modifier-tagging SNP and those SGVs in strong linkage disequilibrium with it ( $R^2 > 0.8$ ; Table S2). From the normal chromosomes from the KGP (phase 3), we then constructed nucleotide-resolution modifier haplotypes representing the consensus alleles of those KGP chromosomes that carry the tag SNPs and delineated protein-altering SGVs. We examined separately those SGVs that were tested in our association analysis and those not tested (Table 1). For example, in the KGP data, 2,836 SGVs are present within the boundaries of modifier haplotype 15AM1; 1,703 of these were imputed

and tested in our SNP association analysis. Among these tested variants, only two SNPs are protein-altering: (1) rs150393409 (MAF = 1.44% in the study subjects; *FAN1* p.Arg507His; annotated as deleterious and possibly damaging in SIFT and PolyPhen, respectively),<sup>20–22</sup> and (2) rs3784588 (MAF = 6.72% in the study subjects; *TRPM1* p.Val1434Ile based on RefSeq accession number NM\_001252020.1; tolerated/benign). Although the former produced the most significant p value in our association analysis ( $p$  value =  $6.7 \times 10^{-29}$  in a fixed model), the latter showed non-genome-wide significance ( $p$  value =  $1.7 \times 10^{-07}$  in a fixed model). In contrast, the KGP data haplotype for the onset-delaying 15AM2 effect did not reveal any alternative alleles that change amino acid sequence at tested variation sites. The 15AM3 modifier haplotype has only one protein-altering variant, the 15AM3-tag SNP rs151322829 (MAF = 0.7% in the study subjects; *FAN1* p.Arg377Trp; deleterious/damaging;  $p$  value =  $9.3 \times 10^{-9}$  in a fixed model). The 15AM5 modifier haplotype carries a protein-altering variant only in *MTMR10* (rs6493352, MAF = 17.4% in the study subjects; p.Arg648His; tolerated/benign;  $p$  value =  $1.3 \times 10^{-04}$  in a fixed model). Of the SNPs listed in the KGP data that were not imputed and thus not tested in our association analysis, none has an alternative allele that is protein-altering on any of the modifier haplotypes.

We also performed targeted DNA capture sequencing analysis<sup>13</sup> of 32 representative HD individuals bearing the 15AM1, 15AM2, 15AM3, and 15AM5 tag SNPs to discover functional variants that might have been missed in our imputed SGV association analysis and in the KGP data analysis (Table 1). Given the frequencies of the tag SNPs, we were able to analyze heterozygotes for 15AM1,

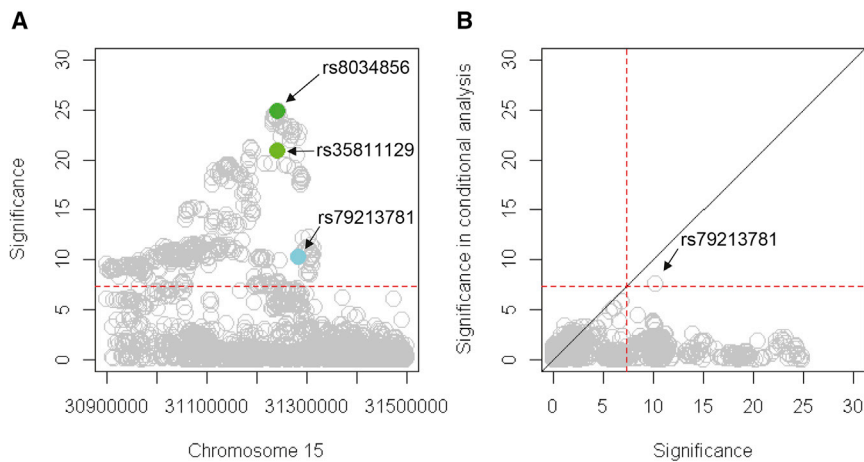


**Figure 2. Refinement of Top Tag SNPs and Identification of an Additional Onset-Hastening Modifier Effect**

(A) To discover additional independent modifier haplotypes, we excluded samples carrying 15AM1 or 15AM3 haplotypes, and we performed association analysis. After drop-out of these infrequent onset-hastening haplotypes, the peak SNP tagging the common onset-delaying 15AM2 haplotype was rs8034856 (dark green circle) rather than the original rs35811129 (light green circle). Interestingly, a relatively infrequent SNP remained significant, suggesting the existence of an independent modifier haplotype tagged by rs79213781 (cyan circle).

(B) To confirm that the modifier effect

tagged by rs79213781 (cyan circle) is independent, the new tag SNP for 15AM2 (rs8034856) was used for conditional analysis of the sample set excluding carriers of 15AM1 or 15AM3. Dotted lines indicate genome-wide significant association.

15AM3, and 15AM5 and homozygotes for 15AM2. Consequently, causal variants were expected to be observed at 50% frequency in the former and at 100% frequency in the latter. Consistent with the GWAS data and functional annotation of modifier haplotypes in KGP data, the capture sequencing confirmed the protein-altering SNPs at expected European ancestry allele frequencies for 15AM1 (rs150393409), 15AM3 (rs151322829), and 15AM5 (rs6493352). Interestingly, one of the subjects who is homozygous for the onset-delaying 15AM2 modifier haplotype was found to harbor a very rare nonsense mutation (rs184745027; FAN1 p.Arg952Ter; MAF = 0.0071% based on gnomAD v2.1.1) in one *FAN1* allele. This subject had onset 11.7 years earlier than expected from their inherited CAG repeat length (CAG = 41; observed age at onset = 44 years; expected age at onset = 55.7 years), consistent with the heterozygous loss of FAN1 function producing an onset-hastening effect. Together, these detailed analyses of the chr15 HD modifier locus point to *FAN1* as the only gene common to all four modifier haplotypes and the only gene with evidence for causal protein sequence alterations, and this suggests in particular that the 15AM1 and 15AM3 modifier effects are due respectively to the FAN1 p.Arg507His and p.Arg377Trp missense variants (Table S3).

### Reduced DNA-binding Activity of 15AM1 and 15AM3 FAN1 Proteins

These postulated causal 15AM1 (p.Arg507His) and 15AM3 (p.Arg377Trp) variants involve amino acids in and near the DNA-binding domain of FAN1 (Figure 3A), respectively, raising the possibility that they affect FAN1 DNA-binding activity. To test this hypothesis, we generated full-length expression constructs for 15AM1 and 15AM2 FAN1 from HD LCLs; we then derived a 15AM3 construct from the 15AM2 construct via site-directed mutagenesis. Sanger sequencing confirmed that these full-length FAN1 expression constructs matched the KGP haplotype and sequence

data, and this enabled us to test the effect of the selected variants on the DNA-binding activity of FAN1. In qualitative *in vitro* assays using wild-type (WT) and FAN1-knockout cells (Figure S6), we confirmed that FAN1 interacts with 3' flap DNA substrate (Figure S7).<sup>16</sup> Quantitative *in vitro* assays (Figure S8) showed that the DNA-binding activities of FAN1 p.Arg507His (15AM1) and FAN1 p.Arg377Trp (15AM3) are significantly reduced compared to the 15AM2 FAN1, and this supports the proposed functional impact of these missense variants (Figure 3B). Reduced binding of FAN1 p.Arg507His (15AM1) and FAN1 p.Arg377Trp (15AM3) was also observed in binding assay using CAG loop-out, although not in a structure-specific fashion (Figures S9 and S10; Figure 3C).

### Functional Consequences of Reduced FAN1 DNA-Binding Activity

We next determined whether the reduced DNA-binding activity of 15AM1 and 15AM3 FAN1 is reflected in a functional impact on cells. We first evaluated whether FAN1 rescued cytotoxicity that was caused in FAN1-deficient HEK293T by MMC.<sup>23</sup> 15AM2 FAN1 significantly rescued cells from this toxicity (Figure 4A) whereas FAN1 p.Arg507His (15AM1) and FAN1 p.Arg377Trp (15AM3) did not. In addition, HD LCLs carrying the 15AM1 modifier showed increased sensitivity to MMC-mediated toxicity and consequently showed reduced viability compared to those with the 15AM2 modifier (Figure 4B; Figure S11); this result demonstrates that this measure of DNA repair function of FAN1 differs by haplotype and further implicates FAN1 variation as the source of the HD modifier effects.

The suggestion that the onset-hastening and onset-delaying modifier effects both act through an altered rate of somatic expansion of the CAG repeat has recently received mixed support from introduction of an *HTT* exon 1 transgene into FAN1-deficient osteosarcoma cells and from FAN1 shRNA suppression in a human iPSC line with a

**Table 1. Reconstructed Onset Modifier Haplotypes Based on KGP Data and Supplemental Capture Sequencing Data****KGP Data: Haplotype-Based Analysis**

Modifier Haplotype	15AM1	15AM2	15AM3	15AM5
Number of tagging SNPs with $R^2 > 0.8$	3	46	3	2
Modifier haplotype boundary (size)	31202961 - 31300677 (97.7 KB)	31184803 - 31285422 (100.6 KB)	31165091 - 31221358 (56.2 KB)	31204637 - 31282611 (77.9 KB)
Number of chromosomes carrying the haplotype	12	400	7	37
Variation sites in KGP in the region	2836	2965	1669	2292
Tested for HD onset modification	1703	1756	936	1379
Site with reference allele	1583	1652	899	1354
Site with alternative allele	120	104	37	25
Protein-altering variants	2 (rs150393409, rs3784588)	0	1 (rs151322829)	1 (rs6493352)
Not tested for HD onset modification	1133	1209	733	913
Sites with reference allele	1132	1203	727	912
Sites with alternative allele	1	6	6	1
Protein-altering variants	0	0	0	0

**Capture Sequencing Data**

Modifier Haplotype	15AM1	15AM2	15AM3	15AM5
Modifier haplotype boundary (size)	31202961 - 31300677 (97.7 KB)	31184803 - 31285422 (100.6KB)	31165091 - 31221358 (56.2 KB)	31204637 - 31282611 (77.9 KB)
Number of QC-passed tagging SNPs	3	36 <sup>a</sup>	3	2
Samples (chromosomes) carrying the haplotype	18 (18)	8 (16)	3 (3)	3 (3)
Expected frequency of casual variant (%)	50	100	50	50
Protein-altering SNP with expected frequency	rs150393409	0	rs151322829	rs6493352
Other exon SNP with expected frequency	0	0	0	0

Since the causal variations responsible for onset modification signals must exist within the region of association, we constructed the consensus haplotype for the chromosomal regions responsible for each of the 4 modifier effects. Panels of modifier haplotype-tagging SNPs (peak SNP + SNPs with  $R^2 > 0.8$ ) were used to define the analysis regions and to identify modifier haplotypes in KGP data for subsequent analysis focusing on functional variants. For example, the 15AM1 consensus haplotype was constructed based on 12 KGP chromosomes identified by 3 15AM1-tagging SNPs. In the region defined by 15AM1-tagging SNPs (chr15: 31202961 - 31300677), 2,836 SNPs are described in the KGP data, and 1,703 of them were tested in our association analysis. Among tested variants, the 15AM1 consensus haplotype carries alternative alleles at 120 sites; 2 of those are annotated as protein-altering variations (rs150393409 and rs3784588). Of 1,133 not-tested variants, the 15AM1 consensus haplotype carries alternative alleles at 1 site (not protein-altering). Independently, representative Huntington disease (HD) samples carrying modifier haplotype-tagging SNPs were sequenced by a targeted capture sequencing method. DNA samples were heterozygous for 15AM1 (18 samples), 15AM3 (3 samples) or 15AM5 (3 samples), or were homozygous for 15AM2 (8 samples). Allele frequencies observed in the sequence data across the modifier haplotypes were compared to the expected allele frequency of the causal variation (50% for heterozygous subjects, 100% for homozygous subjects) focusing on protein-altering variants. Analysis focusing on other exon SNPs that were not annotated in KGP data did not reveal any variants with expected allele frequencies.

<sup>a</sup>Among 46 15AM2-tagging SNPs, 36 SNPs passed QC for capture sequencing analysis.

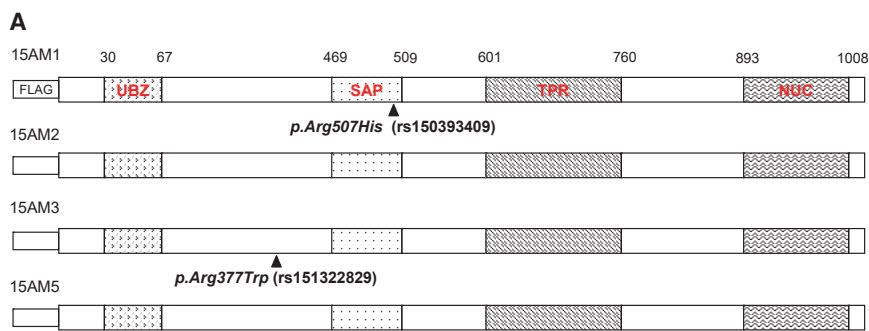
long, inherently unstable CAG repeat (~121 CAGs from a subject with 109 CAG repeats).<sup>12</sup> To confirm that the capacity of FAN1 to influence HD onset is reflected in its ability to suppress somatic *HTT* CAG expansion at the endogenous *HTT* locus in a subject whose CAG repeat does not show dramatic modal size increase in culture, we completely inactivated *FAN1* through the use of CRISPR/Cas9 editing in an HD iPSC line with 73 CAG repeats. The result, as assessed from the calculated expansion index<sup>19</sup> of dividing iPSC clonal lines, was a gradual increase in the appearance of CAG repeats larger than the starting modal length over the course of continued culture

(Figure 4C; Figure S12); this result indicates that FAN1 normally functions to stabilize the expanded CAG repeat.

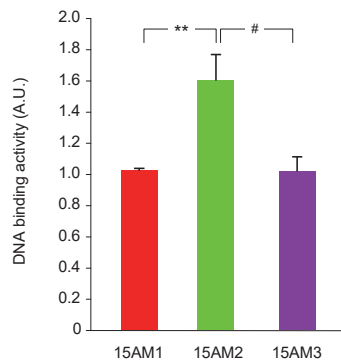
### Effects of Modifier Haplotypes on *FAN1* Expression Levels

In the recent GWAS publication, we reported correlations between the modification signals from 15AM2 (not 15AM1 or 15AM3) and *FAN1* eQTL signals in the cortex subset of the GTEx Consortium data.<sup>10</sup> We have not observed similar correlations for *MTMR10* or *TRPM1* eQTL signals (data not shown). To confirm in a larger data set that altered expression of *FAN1* could explain

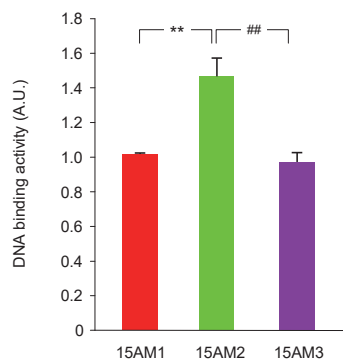




**B** Binding to 3' flap DNA substrate



**C** Binding to a CAG loop-out structure



repeat, and virus type replication repair nuclease, respectively. Diagrams of haplotypes were focused on *FAN1* because modifier haplotype-specific variations do not alter protein sequence or are not associated with expression levels of other nearby genes (e.g., *MTMR10*, *TRPM1*).

(B) DNA-binding activities of the 3 different *FAN1* proteins were determined by *in vitro* assays using 3' flap comprising a set of 3 oligos. FLAG-tagged *FAN1* protein nuclear extract and biotinylated oligos were incubated, and the protein-oligo complex was pulled down by streptavidin. The amount of *FAN1* was quantified by immunoblot analysis using *FAN1* antibody, and data were normalized by the amount of *FAN1* in the inputs. DNA-binding activity on the Y-axis represents densitometry reading of pull-down divided by that of input for each group (A.U., arbitrary unit). Five independent experiments were summarized (5 technical replicates/group).

(C) Similarly, DNA-binding activity of *FAN1* was determined using oligos of 10 CAG loop-out (potentially forming 5 CAG long hairpin/loop structure). Experiments were repeated three times (3 technical replicates/group). Error bars represent the standard errors.

\*p value < 0.05; \*\*p value < 0.01.

some modifier effects, we performed eQTL analysis using the CMC data. As shown in Figure 5, genome-wide significant eQTL signals for *FAN1* were generated by SNPs tagging the 15AM2 haplotype but not by those tagging the 15AM1, 15AM3, or 15AM5 modifier haplotypes. In agreement with these observations, co-localization analysis of HD modifier association data and CMC eQTL data showed posterior probabilities for the effects sharing the same causal variant of 97.0% for SNPs tagging 15AM2. In contrast, 15AM1-, 15AM3-, and 15AM5-tagging SNPs revealed posterior probabilities of 8.3%, 8.5%, and 9.8%, respectively, for the HD modifier and eQTL effects sharing the same causal variant (Figure 5C). Comparison of the directions of the eQTL and onset modification signals confirmed that the onset-delaying 15AM2 modifier effect is associated with a relative increase in the level of *FAN1* mRNA expression.

Additional analyses for *FAN1* did not reveal any compelling evidence supporting a role for splicing as a genetic modifier of HD (GTEx portal). Taken together, the haplo-

### Figure 3. *FAN1* Missense Variants on 15AM1 and 15AM3 Modifier Haplotypes Reduce DNA Binding

(A) Through sequence analysis, we fully reconstructed *FAN1* modifier haplotypes at the levels of nucleotide and amino acid. Subsequently, LCLs from representative HD patients were used for cDNA cloning to generate full-length mammalian expression constructs for the modifier haplotypes 15AM1 and 15AM2. Because (1) cell lines carrying the modifier haplotype 15AM3 were not readily available due to low allele frequency, and (2) the modifier haplotype 15AM3 differs from 15AM2 at one nucleotide, site-directed mutagenesis was performed to generate the expression vector for 15AM3. The *FAN1* sequence of 15AM5 is identical to that of 15AM2, and therefore the effects of 15AM5 modifier *FAN1* can be tested by using the 15AM2 modifier *FAN1* construct (second diagram). Each construct has a FLAG tag at the N-terminus for biochemical assays. Subsequent sequencing analysis of expression constructs confirmed the DNA sequence reconstructed by KGP data analysis and capture sequencing. Black triangles indicate deleterious and/or damaging missense variations. Domains are shown: UBZ, SAP, TPR, and NUC represent ubiquitin-binding Zinc finger, SAF-AIB, Acinus, and PIAS (DNA-binding domain), tetratricopeptide

type and sequencing data and the eQTL analyses support the suspected role of *FAN1* as the gene responsible for the four independent modifier signals on chr15, with the causal variants on the 15AM1 and 15AM3 modifiers likely being the *FAN1* missense changes, rs150393409 and rs151322829, respectively, and the 15AM2 modifier acting through alteration of *FAN1* mRNA levels. The mechanism by which the 15AM5 modifier acts is not clear and requires further investigation.

### Effect of Modifier Genotype on Age at Onset Modification

The individual SNP association analyses as performed in the GWA studies are based upon the assumption of additivity across major allele homozygotes and heterozygotes and minor allele homozygotes. Once the modifier haplotypes were defined, it became possible to use the tag SNPs to test whether the mechanisms underlying the modifier effects at this particular locus, which include both structural changes to *FAN1* and differences in mRNA

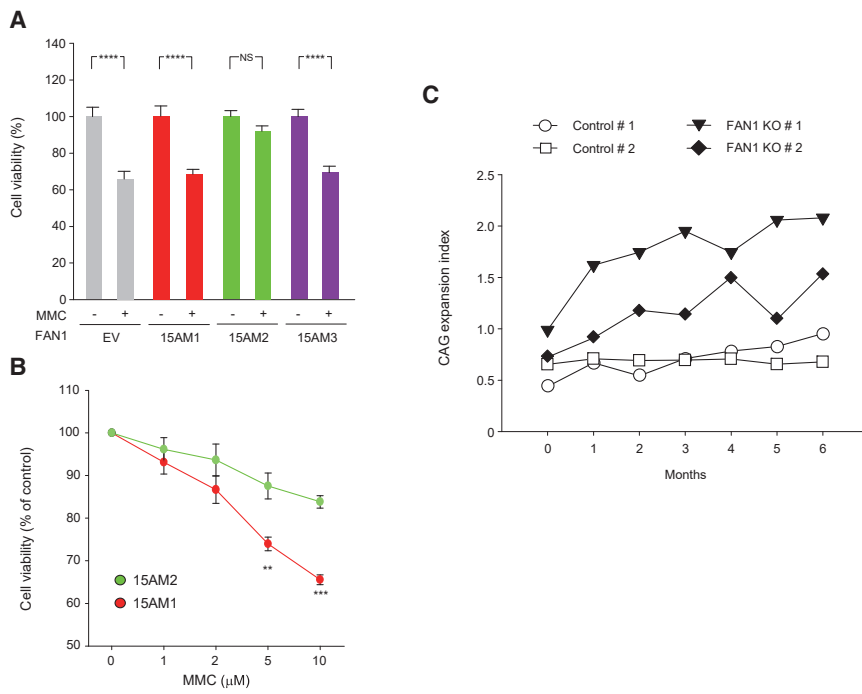


**Figure 4. Reduced Rescue from MMC-Mediated Toxicity by 15AM1 and 15AM3** (A) *FAN1* knockout HEK293T cells were used to determine the levels of rescue afforded by over-expression of different *FAN1* haplotypes. *FAN1* knockout HEK293T cells were treated with either vehicle (-) or MMC (+; 10 μM for 24 h), and then viability assays were performed to determine the levels of rescue from the MMC-induced cytotoxicity. Viability in the absence of MMC treatment was considered as 100% (i.e., control) for each experimental group. Error bars represent standard errors (12 technical replicates/condition from 3 independent experiments). NS, not significant

(B) LCLs derived from HD subjects carrying either 15AM1 (red; 5 lines, all heterozygous for 15AM1) or 15AM2 modifier *FAN1* (green; 3 and 2 lines heterozygous and homozygous for the 15AM2, respectively) were treated with various concentrations of MMC to determine viability by Cell Titer-Glo assay. Vehicle treated cells were used as controls. We hypothesized that the expression levels of *FAN1* in cells were similar due to the lack of a significant

*FAN1* eQTL in LCL (Figure S11). LCLs with 15AM3 were not available due to the low frequency of the haplotype, and therefore were not tested. Error bars represent standard errors (5 biological replicates/group, 24 technical replicates/condition for each biological replicate from 4 independent experiments). \*\*, p value < 0.01; \*\*\*, p value < 0.001; \*\*\*\*, p value < 0.0001 by Student's t-test.

(C) *FAN1* was knocked out in iPSC derived from a HD subject (carrying 72/15 CAGs and two copies of 15AM2 modifier haplotype) by CRISPR/Cas9. Subsequently, 2 clonal lines for *FAN1* knockout (KO; starting modal CAGs 75 and 72, respectively) and 2 control lines (empty vector treated; starting modal CAGs 74 and 73, respectively) were established. These cells were maintained in standard iPSC culture conditions, and DNA samples were collected longitudinally and analyzed by PCR sizing to calculate expansion index. Thus, these data represent the levels of CAG repeat instability in proliferating iPSC, not differentiated neurons. Each data point represents a single measurement. Fluctuations seen in KO clones (#1 at 4 months and #2 at 5 months) might be due to the possibility that some of expanded alleles were filtered out by 10% peak height threshold in our expansion index quantification procedure because of low PCR amplification efficiencies in corresponding samples.

expression level in cortex, are indeed additive or, alternatively, show evidence of non-additive effects. Of the 9,058 GWA study subjects, 3,868 (42.7%) carried a haplotype other than 15AM1, 15AM2, 15AM3, or 15AM5 (i.e., a non-modifier or "Other" haplotype based on the four top tag SNPs), most frequently as a heterozygote with one of the modifier haplotypes (Table 2). We first determined the effect size attributable to one copy of 15AM1, 15AM2, 15AM3, or 15AM5 by (1) selecting HD GWA subjects who each had one chromosome bearing the minor allele of the corresponding haplotype tag SNP and one chromosome with only major alleles at all four tag SNPs (i.e., a non-modifier chromosome or "Other" in Table 2) and then (2) comparing their residual age at onset to individuals who each bear only two non-modifier chromosomes, with the difference in the respective residuals constituting the effect attributable to the modifier haplotype.

Having determined the effect size for a single copy of each modifier allele, we were then able to examine individuals who each carry two modifier chromosomes. Under the additive model, for any given diplotype, the expected residual age at onset can be predicted by simply adding the individual effect sizes of the haplotypes repre-

sented. Diplotypes that included 15AM2, which is reasonably frequent, showed no significant deviation (Student's t-test, p value = 0.9175) from the additivity-based expectation (Table 2); this result indicates that each copy of 15AM2, which appears to act as an onset-delaying modifier through increased *FAN1* expression in the cortex, has its effect independently of whether the other chromosome 15 bears another 15AM2 copy, a copy of one of the onset-hastening modifiers, or a non-modifier version of the locus.

All other combinations of modifier haplotypes (involving either homozygosity or compound heterozygosity for onset-hastening modifiers) are infrequent (Table 2). All showed a residual age at onset that is more negative than expected (i.e., even earlier onset than predicted by additivity of the effects), a difference that over the entire group is statistically significant (Student's t-test, p value = 0.03162). The fact that absence of any non-modifier *FAN1* in an individual (i.e., two onset hastening-haplotypes) produces a worse outcome than predicted from onset-hastening modifier heterozygotes indicates that the presence of a non-modifier *FAN1* locus does act to mitigate to some degree the effect of the onset-hastening modifiers. The sample size for this group is small and therefore

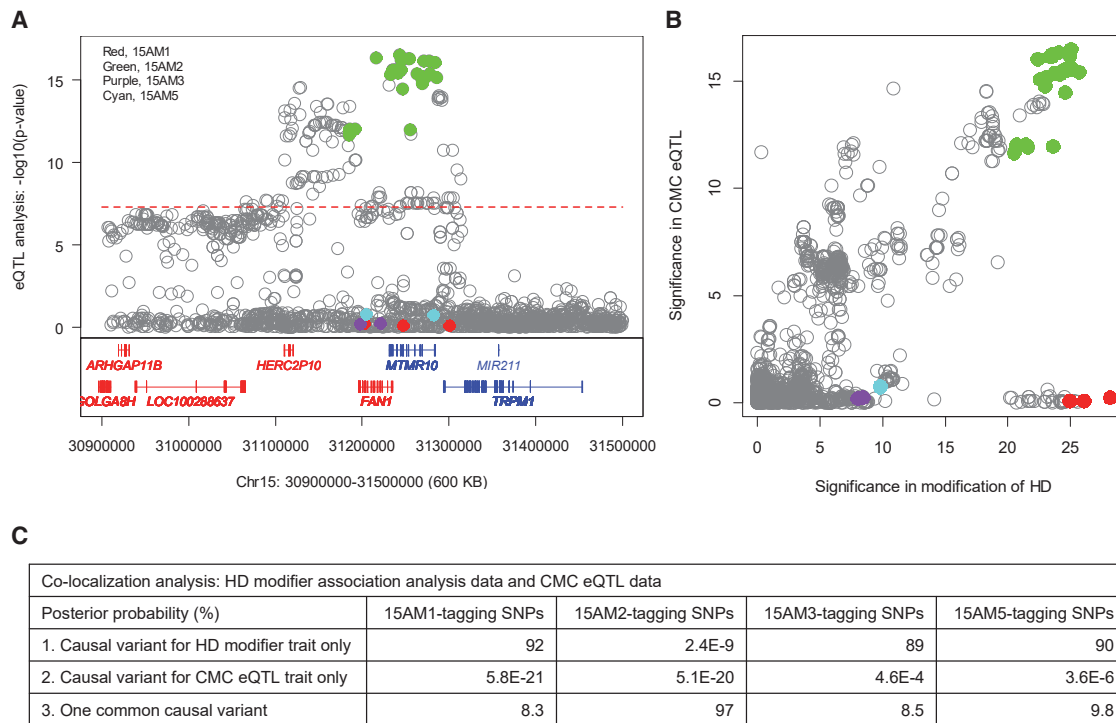


**Figure 5. Co-localization of 15AM2 Modification Signals and *FAN1* eQTL Signals**

(A) eQTL analysis was performed using RNAseq and genotype data sets from the CMC, focusing on *FAN1*. Expression levels of *FAN1* were modeled as a function of a test SNP and covariates in a fixed-effect model. Y-axis and X-axis represents significance in eQTL analysis (i.e.,  $-\log_{10}(p \text{ value})$ ) and genomic location (GRCh 37/hg19), respectively. Haplotype-tagging SNPs are indicated by colored symbols (red, 15AM1, green, 15AM2; purple, 15AM3; cyan, 15AM5).

(B) Signals (i.e.,  $-\log_{10}(p \text{ value})$ ) in HD modifier GWA data (X-axis) and CMC *FAN1* eQTL data (Y-axis) were compared for shared SNPs between two data sets.

(C) Co-localization analysis was performed using modifier association data and *FAN1* eQTL data of haplotype-tagging SNPs. Percent posterior probability was calculated for 1) causal variant for HD onset modification only, 2) causal variant for *FAN1* eQTL only, and 3) common causal variant for both HD onset modification and *FAN1* eQTL using haplotype-tagging SNPs.

additional samples will be needed to replicate this finding and to examine the behavior of the individual onset-hastening modifier haplotypes.

## Discussion

Our GWAS study of HD age at onset identified multiple modifier loci that remarkably, at or near the peak association signal, had the presence of a gene involved in DNA maintenance processes; this suggests that these genes are the sources of HD modification. At the 15q13.2–13.3 locus, the corresponding candidate gene was *FAN1*, which encodes a protein that is involved in repair of ICL-induced DNA breaks, cleaving DNA at every third nucleotide from a cut end by using its 5′–3′ exonuclease activity.<sup>16</sup> Further, while *FAN1* does not participate in DNA double-strand break resection, *FAN1* is required for efficient homologous recombination.<sup>22,24</sup> Consequently, in order to guide strategies for therapeutic intervention and provide genetic guidance for clinical trial design, we set out to establish whether *FAN1* is indeed the modifier gene at this locus. Taken together, our genetic and molecular data confirm that *FAN1* is the source of the chr15 locus modifier effect

in HD and strongly point to altered *FAN1* DNA-binding activity (15AM1, 15AM3) and expression level (15AM2) as sources of onset-hastening and onset-delaying modification, respectively. Interestingly, the p.Arg507His and p.Arg377Trp variants associated with the 15AM1 and 15AM3 HD modifier effects were reported originally in families with early-onset breast cancer,<sup>25</sup> but, despite a plausible argument for *FAN1* function playing a role in tumorigenesis, these substitutions are not associated with increased risk of breast cancer in the general population. There is, however, evidence for a functional impact *in vivo*: the p.Arg507His substitution on 15AM1 has recently been associated in genetic studies with karyomegalic interstitial nephritis, a recessively inherited disease caused by loss of *FAN1* function.<sup>26</sup> Our genetic data also indicate that some as yet undetermined mechanism other than a protein-altering variant can also result in earlier than expected onset (15AM5). Finally, the previously named haplotype 15AM4<sup>10</sup> does not represent a single independent modifier effect, but rather combinations of the effects of the 15AM1, 15AM2, 15AM3, and 15AM5 haplotypes.

The mirrored effects of reduced function (reduced DNA-binding activity of 15AM1 and 15AM3) and increased expression (15AM2) of *FAN1* on the timing of HD onset

**Table 2. Test Whether Combinations of Two Modifier Haplotypes Are Additive or Synergistic**

<b>Subjects with One Modifier Haplotype and Effect Size Estimation</b>				
1 <sup>st</sup> Chr	2 <sup>nd</sup> Chr	n	Observed Residual (Years)	Effect Size (Years)
other	other	3,868	-0.55	Baseline
15AM1	other	164	-5.02	15AM1 : -4.47
15AM2	other	3,621	0.64	15AM2 : 1.19
15AM3	other	89	-3.90	15AM3 : -3.35
15AM5	other	227	-2.72	15AM5 : -2.17
<b>Effects of Selected Modifier Haplotypes in the Presence of 15AM2</b>				
1 <sup>st</sup> Chr	2 <sup>nd</sup> Chr	n	Observed Residual (Years)	Expected Residual (Years)
15AM1	15AM2	85	-4.21	-3.83
15AM2	15AM2	851	1.81	1.83
15AM3	15AM2	30	-2.92	-2.71
15AM5	15AM2	105	-1.69	-1.53
Student's t-test, p value = 0.9175				
<b>Subjects with Two Onset-Hastening Modifier Haplotypes</b>				
1 <sup>st</sup> Chr	2 <sup>nd</sup> Chr	n	Observed Residual (Years)	Expected Residual (Years)
15AM1	15AM1	1	-21.76	-9.49
15AM1	15AM3	2	-13.40	-8.37
15AM1	15AM5	6	-9.38	-7.19
15AM3	15AM3	2	-10.83	-7.25
15AM3	15AM5	1	-15.57	-6.07
15AM5	15AM5	6	-8.13	-4.89
Student's t-test, p value = 0.03162				

To estimate the effect size of each modifier (top section), we identified Huntington disease (HD) subjects carrying only one copy of either 15AM1, 15AM2, 15AM3, or 15AM5, and we compared them with HD subjects who did not carry any of these modifier haplotypes ("Other" group as the baseline). For example, the effect size of 15AM1 was calculated by subtracting the observed residual age at onset of the "Other" group from that of HD subjects carrying one copy of the 15AM1 modifier haplotype. n represents the number of HD subjects.

We then determined whether the onset-delaying effect of a single 15AM2 chromosome is influenced by the presence of a second modifier haplotype (middle section). Expected residual age at onset of each group was based on the effect sizes estimated in the top section.

Finally, a small number of HD subjects carry two copies of infrequent onset-hastening modifier haplotypes (i.e., 15AM1, 15AM3, and 15AM5; bottom section). To determine whether two onset-hastening modifier haplotypes generate non-additive effects, we compared the residual age at onset based upon addition of effect sizes from the top section to observed residuals. Student's t-tests were performed to determine whether observed residuals and expected residuals were significantly different.

suggest that a process involving FAN1 could represent a therapeutic target for slowing HD pathogenesis. In addition to *FAN1*, several other genes associated with DNA maintenance processes, including *MLH1*, *MSH3*, *PMS1*, *PMS2*, and *LIG1*, map in the vicinity of HD modifier GWAS signals on other chromosomes. The modifying effects of such DNA maintenance genes could theoretically influence HD pathogenesis by modulating accumulated DNA damage across the genome. However, the fact that the timing of HD onset is determined by a property of the CAG repeat, rather than by continuous polyglutamine toxicity, favors a model in which these genetic modifiers act on the CAG repeat to alter its rate of somatic expansion. A role for *FAN1* in the process of CAG repeat expansion has been supported by recent studies of an HD exon 1 mini-gene in *FAN1* knockout osteosarcoma cells, where CAG repeats of 30 and 70 CAGs Chr were stable while modal repeats of

97 and 118 showed an increase in size during 40 days of culture.<sup>12</sup> The osteosarcoma cell assay did not distinguish the effects of WT *FAN1*, p.Arg507His variant *FAN1*, or a nuclease-inactive variant of *FAN1* when each of these was introduced via expression construct; this result suggests that expression at endogenous levels or for a longer period of time might be required to assess a functional impact of the missense variant on expansion. Alternatively, *FAN1*'s participation in the mechanism of repeat instability may not be precisely the same in dividing cells and in non-dividing post-mitotic neurons. For example, the minor allele at *FAN1* rs3512 is associated with increased repeat expansion in the blood cells of HD subjects,<sup>27</sup> but, as part of the 15AM2 haplotype, it is associated with delayed age at onset and a suspected decrease in CAG expansion in neurons. Consequently, it remains unclear whether *FAN1* acts in neurons through its ICL-resolving

role or through some other function in DNA maintenance processes.

Although in our assays a difference in DNA binding for FAN1 containing either of the two missense variants was readily detectable in transfected cells, and LCLs with these mutations showed increased sensitivity to MMC, we focused our assessment of CAG expansion on the endogenous repeat in clonal HD patient-derived iPSCs from a subject with 73 CAGs. As monitored by our established expansion index measure,<sup>19</sup> in iPSCs with intact *FAN1* alleles, this starting repeat was relatively stable through the relatively short 6 month culture assay, as might be expected from the multi-year time course of somatic expansion postulated to lead *in vivo* to clinical onset in HD subjects. In parallel isogenic lines with no FAN1 due to CRISPR/Cas9-mediated inactivation, we observed a slow, gradual increase in expansion index. A more exaggerated response has been seen in another human HD iPSC line with a longer, inherently unstable repeat, where ongoing CAG expansion was increased by partial FAN1 shRNA knock-down.<sup>12</sup> Taken together with the increased expression level associated with the 15AM2 modifier and its onset-delaying effect, these studies argue that WT FAN1 functions to suppress CAG repeat expansion, a conclusion that also supports the candidacy of FAN1 as a potential modifier of other CAG repeat disorders<sup>28</sup> and, as suggested in a recent report that *Fan1* knockout enhances somatic expansion of CGG repeats in a model of Fragile X disorders,<sup>11</sup> implies a role for FAN1 more broadly in triplet repeat diseases.

A role for FAN1 in suppressing somatic CAG expansion, combined with the onset-delaying effect of the 15AM2 modifier haplotype, suggest that increasing the expression of WT *FAN1* could have therapeutic benefit in delaying the onset of HD. The additivity of the 15AM2 effect in the presence of either a second 15AM2 allele or a 15AM1, 15AM3, or 15AM5 allele indicates that such a treatment could be widely applicable. Increased *FAN1* expression could theoretically be achieved by upregulating an endogenous allele, but this would require that the subject expresses a WT coding sequence from at least one allele. It is also not certain whether this upregulation would have to be chromosome-specific, since we cannot assess from the population analysis any potential negative effect of upregulating the 15AM1, 15AM3, or 15AM5 chromosomes. An alternative strategy would be to introduce exogenous FAN1, which might be particularly effective for subjects with two onset-hastening modifiers. Even if *FAN1* expression is not the mechanism chosen for therapeutic intervention, knowledge of the *FAN1* diplotype in an HD subject can be of potential importance for designing clinical trials of other mechanisms of intervention. For any trial in which conversion from premanifest to manifest disease is used as a measure, incorporating the *FAN1* genotype and its onset-modifying effect could either guide selection of trial subjects or provide greater precision in calculating the effect of treatment. Similarly, the *FAN1* genotype may be useful in the premanifest phase of HD, where it has been

shown to influence measures such as putamen volume and symbol digits modalities test score.<sup>29</sup> Whether the *FAN1* genotype also influences the rate of progression of individual measures in manifest disease subjects and could be used in early HD trials remains to be determined. Additionally, if the intervention being tested is aimed specifically at blocking the process of somatic CAG expansion, then the *FAN1* genotype and knowledge of any potential genetic interactions with other HD modifier genes that might interfere with or enhance the ability to reliably measure outcomes will also be crucial.

HD is a devastating disorder without treatments that are effective in delaying onset or slowing the worsening of disease manifestations. We undertook the characterization of genetic modifiers that alter the course of the human disease as a potential route to effective mechanism-based treatments. The accumulated evidence supporting *FAN1* as the HD modifier gene at the 15q13.2–13.3 locus reinforces the view that each of the DNA maintenance genes at or near modifier signals on chromosomes 2 (*PMS1*), 3 (*MLH1*), 5 (*MSH3*), 7 (*PMS2*), and 19 (*LIG1*) will prove to be the respective sources of HD modification through influences on somatic expansion of the CAG repeat. Similarly, these findings suggest that other GWA loci without known DNA maintenance genes may point to genes that also participate in the CAG repeat expansion process even though they are not currently recognized as being involved in DNA repair (e.g., *RRM2B* on chromosome 8 and *CCDC82* on chromosome 11). The success of this GWAS strategy as applied to the timing of HD onset dictates that this approach also be applied to other landmarks in the HD disease process and to the rate of worsening disease, particularly during the period of early manifest HD most applicable to clinical trials, in order to maximize the opportunity to identify therapeutic targets for effective treatments that alleviate the suffering of families with this devastating disease.

### Supplemental Data

Supplemental Data can be found online at <https://doi.org/10.1016/j.ajhg.2020.05.012>.

### Acknowledgements

We are grateful to Huntington disease families and clinicians who participate in HD genetic research. This research was funded by National Institutes of Health (NIH) National Institute of Neurological Disorders and Stroke (NINDS) grants NS091161, NS105709, and NS049206, by an anonymous donor, and by the Cure Huntington's Disease Initiative (CHDI) Foundation.

### Declaration of Interests

J.F.G. is a Scientific Advisory Board member and has a financial interest in Triplet Therapeutics. His NIH-funded project is using genetic and genomic approaches to uncover other genes that significantly influence when diagnosable symptoms emerge and how

rapidly they worsen in Huntington disease. The company is developing new therapeutic approaches to address triplet repeat disorders such as Huntington disease, myotonic dystrophy, and spinocerebellar ataxias. His interests were reviewed and are managed by Massachusetts General Hospital and Partners HealthCare in accordance with their conflict of interest policies.

### Data Availability

The original summary statistics of the GeM-HD genome-wide association study to identify genetic modifiers of HD can be obtained at <https://datadryad.org/stash/dataset/doi:10.5061/dryad.5d4s2r8>.

Received: March 18, 2020

Accepted: May 18, 2020

Published: June 25, 2020

### Web Resources

1000 Genomes Project data, <https://www.internationalgenome.org/>  
CommonMind Consortium, <https://www.synapse.org/#!Synapse:syn2759792/wiki/69613>  
ExAC, <http://exac.broadinstitute.org/>  
GeCKO, <http://genome-engineering.org/gecko/>  
Genome Analysis Toolkit, <https://gatk.broadinstitute.org/hc/en-us>  
gnomeAD, <https://gnomad.broadinstitute.org/>  
Michigan Imputation Server, <https://imputationserver.sph.umich.edu/index.html>  
MIT CRISPR design website, <https://zlab.bio/guide-design-resources>  
OMIM, <https://www.omim.org>  
PENNCNV, <http://penncnv.openbioinformatics.org/en/latest/>  
PLINK, <http://zzz.bwh.harvard.edu/plink/>  
sQTL analysis in the GTEx portal, <https://gtexportal.org/home/spliceQTLPage>

### References

1. The Huntington's Disease Collaborative Research Group (1993). A novel gene containing a trinucleotide repeat that is expanded and unstable on Huntington's disease chromosomes. *Cell* 72, 971–983.
2. Bates, G.P., Dorsey, R., Gusella, J.F., Hayden, M.R., Kay, C., Leavitt, B.R., Nance, M., Ross, C.A., Scahill, R.I., Wetzel, R., et al. (2015). Huntington disease. *Nat. Rev. Dis. Primers* 1, 15005. <https://doi.org/10.1038/nrdp.2015.5>.
3. Keum, J.W., Shin, A., Gillis, T., Mysore, J.S., Abu Elneel, K., Lucente, D., Hadzi, T., Holmans, P., Jones, L., Orth, M., et al. (2016). The HTT CAG-Expansion Mutation Determines Age at Death but Not Disease Duration in Huntington Disease. *Am. J. Hum. Genet.* 98, 287–298.
4. Andrew, S.E., Goldberg, Y.P., Kremer, B., Telenius, H., Theilmann, J., Adam, S., Starr, E., Squitieri, F., Lin, B., Kalchman, M.A., et al. (1993). The relationship between trinucleotide (CAG) repeat length and clinical features of Huntington's disease. *Nat. Genet.* 4, 398–403.
5. Duyao, M., Ambrose, C., Myers, R., Novelletto, A., Persichetti, F., Frontali, M., Folstein, S., Ross, C., Franz, M., Abbott, M., et al. (1993). Trinucleotide repeat length instability and age of onset in Huntington's disease. *Nat. Genet.* 4, 387–392.
6. Lee, J.M., Ramos, E.M., Lee, J.H., Gillis, T., Mysore, J.S., Hayden, M.R., Warby, S.C., Morrison, P., Nance, M., Ross, C.A., et al.; PREDICT-HD study of the Huntington Study Group (HSG); REGISTRY study of the European Huntington's Disease Network; HD-MAPS Study Group; and COHORT study of the HSG (2012). CAG repeat expansion in Huntington disease determines age at onset in a fully dominant fashion. *Neurology* 78, 690–695.
7. Persichetti, F., Srinidhi, J., Kanaley, L., Ge, P., Myers, R.H., D'Arrigo, K., Barnes, G.T., MacDonald, M.E., Vonsattel, J.P., Gusella, J.F., et al. (1994). Huntington's disease CAG trinucleotide repeats in pathologically confirmed post-mortem brains. *Neurobiol. Dis.* 1, 159–166.
8. Correia, K., Harold, D., Kim, K.H., Holmans, P., Jones, L., Orth, M., Myers, R.H., Kwak, S., Wheeler, V.C., MacDonald, M.E., et al. (2015). The Genetic Modifiers of Motor Onset Age (GeM MOA) Website: Genome-wide Association Analysis for Genetic Modifiers of Huntington's Disease. *J. Huntingtons Dis.* 4, 279–284.
9. Genetic Modifiers of Huntington's Disease (GeM-HD) Consortium (2015). Identification of Genetic Factors that Modify Clinical Onset of Huntington's Disease. *Cell* 162, 516–526.
10. Genetic Modifiers of Huntington's Disease Consortium; and Genetic Modifiers of Huntington's Disease (GeM-HD) Consortium (2019). CAG Repeat Not Polyglutamine Length Determines Timing of Huntington's Disease Onset. *Cell* 178, 887–900 e814.
11. Zhao, X.N., and Usdin, K. (2018). FAN1 protects against repeat expansions in a Fragile X mouse model. *DNA Repair (Amst.)* 69, 1–5.
12. Gool, R., Flower, M., Moss, D.H., Medway, C., Wood-Kaczmar, A., Andre, R., Farshim, P., Bates, G.P., Holmans, P., Jones, L., and Tabrizi, S.J. (2019). FAN1 modifies Huntington's disease progression by stabilizing the expanded HTT CAG repeat. *Hum. Mol. Genet.* 28, 650–661.
13. Chao, M.J., Kim, K.H., Shin, J.W., Lucente, D., Wheeler, V.C., Li, H., Roach, J.C., Hood, L., Wexler, N.S., Jardim, L.B., et al. (2018). Population-specific genetic modification of Huntington's disease in Venezuela. *PLoS Genet.* 14, e1007274.
14. Sanjana, N.E., Shalem, O., and Zhang, F. (2014). Improved vectors and genome-wide libraries for CRISPR screening. *Nat. Methods* 11, 783–784.
15. Shalem, O., Sanjana, N.E., Hartenian, E., Shi, X., Scott, D.A., Mikkelsen, T., Heckl, D., Ebert, B.L., Root, D.E., Doench, J.G., and Zhang, F. (2014). Genome-scale CRISPR-Cas9 knockout screening in human cells. *Science* 343, 84–87.
16. Wang, R., Persky, N.S., Yoo, B., Ouerfelli, O., Smogorzewska, A., Elledge, S.J., and Pavletich, N.P. (2014). DNA repair. Mechanism of DNA interstrand cross-link processing by repair nuclease FAN1. *Science* 346, 1127–1130.
17. Deng, W.G., Zhu, Y., Montero, A., and Wu, K.K. (2003). Quantitative analysis of binding of transcription factor complex to biotinylated DNA probe by a streptavidin-agarose pulldown assay. *Anal. Biochem.* 323, 12–18.
18. Consortium, H.D.I. (2012). Induced pluripotent stem cells from patients with Huntington's disease show CAG-repeat-expansion-associated phenotypes. *Cell stem cell* 11, 264–278.
19. Lee, J.M., Zhang, J., Su, A.I., Walker, J.R., Wiltshire, T., Kang, K., Dragileva, E., Gillis, T., Lopez, E.T., Boily, M.J., et al.

- (2010). A novel approach to investigate tissue-specific trinucleotide repeat instability. *BMC Syst. Biol.* 4, 29.
20. O'Donnell, L., and Durocher, D. (2010). DNA repair has a new FAN1 club. *Mol. Cell* 39, 167–169.
  21. Smogorzewska, A., Desetty, R., Saito, T.T., Schlabach, M., Lach, F.P., Sowa, M.E., Clark, A.B., Kunkel, T.A., Harper, J.W., Colaiácovo, M.P., and Elledge, S.J. (2010). A genetic screen identifies FAN1, a Fanconi anemia-associated nuclease necessary for DNA interstrand crosslink repair. *Mol. Cell* 39, 36–47.
  22. MacKay, C., Déclais, A.C., Lundin, C., Agostinho, A., Deans, A.J., MacArtney, T.J., Hofmann, K., Gartner, A., West, S.C., Helleday, T., et al. (2010). Identification of KIAA1018/FAN1, a DNA repair nuclease recruited to DNA damage by monoubiquitinated FANCD2. *Cell* 142, 65–76.
  23. Hlavín, E.M., Smeaton, M.B., and Miller, P.S. (2010). Initiation of DNA interstrand cross-link repair in mammalian cells. *Environ. Mol. Mutagen.* 51, 604–624.
  24. Kratz, K., Schöpf, B., Kaden, S., Sandoel, A., Eberhard, R., Lademann, C., Cannavó, E., Sartori, A.A., Hengartner, M.O., and Jiricny, J. (2010). Deficiency of FANCD2-associated nuclease KIAA1018/FAN1 sensitizes cells to interstrand crosslinking agents. *Cell* 142, 77–88.
  25. Park, D.J., Odefrey, F.A., Hammet, F., Giles, G.G., Baglietto, L., Abcfs, Mccs, Hopper, J.L., Schmidt, D.F., Makalic, E., et al.; ABCFS; and MCCS (2011). FAN1 variants identified in multiple-case early-onset breast cancer families via exome sequencing: no evidence for association with risk for breast cancer. *Breast Cancer Res. Treat.* 130, 1043–1049.
  26. Bastarache, L., Hughey, J.J., Hebring, S., Marlo, J., Zhao, W., Ho, W.T., Van Driest, S.L., McGregor, T.L., Mosley, J.D., Wells, Q.S., et al. (2018). Phenotype risk scores identify patients with unrecognized Mendelian disease patterns. *Science* 359, 1233–1239.
  27. Ciosi, M., Maxwell, A., Cumming, S.A., Hensman Moss, D.J., Alshammari, A.M., Flower, M.D., Durr, A., Leavitt, B.R., Roos, R.A.C., Holmans, P., et al.; TRACK-HD team; and Enroll-HD team (2019). A genetic association study of glutamine-encoding DNA sequence structures, somatic CAG expansion, and DNA repair gene variants, with Huntington disease clinical outcomes. *EBioMedicine* 48, 568–580.
  28. Bettencourt, C., Hensman-Moss, D., Flower, M., Wiethoff, S., Brice, A., Goizet, C., Stevanin, G., Koutsis, G., Karadima, G., Panas, M., et al.; SPATAX Network (2016). DNA repair pathways underlie a common genetic mechanism modulating onset in polyglutamine diseases. *Ann. Neurol.* 79, 983–990.
  29. Long, J.D., Lee, J.M., Aylward, E.H., Gillis, T., Mysore, J.S., Abu Elneel, K., Chao, M.J., Paulsen, J.S., MacDonald, M.E., and Gusella, J.F. (2018). Genetic Modification of Huntington Disease Acts Early in the Prediagnosis Phase. *Am. J. Hum. Genet.* 103, 349–357.